



Micromachining of Carbon Fiber Reinforced Plastics Using Femtosecond Pulsed Laser

Yuhei Konishi¹ · Jiwang Yan²

Received: 23 November 2024 / Revised: 15 March 2025 / Accepted: 18 March 2025
© The Author(s) 2025

Abstract

Microscale grooves and holes were fabricated in carbon fiber reinforced plastics (CFRPs) using femtosecond pulsed laser irradiation, and the characteristics and mechanisms of laser processing were investigated. The relationship between laser fluence and ablation depth was established by measuring the cross-sectional profiles of the microgrooves produced at different laser fluences. Furthermore, the effect of the angle between the edge of the micro holes and the carbon fibers was examined by analyzing the edges and wall surfaces of circular and rectangular holes. Experimental results revealed that the laser processing mechanism was strongly dependent on fiber orientation due to significant heat conduction along carbon fibers. The findings of this study contribute to a deeper understanding of the ultrashort pulsed laser processing characteristics and mechanisms for creating small holes in CFRPs and emphasize the possibility of drilling high-precision holes that can be used in the direct bonding of sensors/IC chips to CFRPs.

Highlights

1. The carbon fiber direction strongly affects the laser micromachining behavior due to the anisotropy in thermal conduction.
2. The machined surface becomes uneven when the directions of carbon fiber and laser scanning path are perpendicular.
3. Submillimeter-size round holes, rectangular blind holes and through-holes were successfully fabricated with high precision.

Keywords Ultrashort pulsed laser · Carbon fiber reinforced plastics · Micromachining · Heat conduction · Heat-affected zone

1 Introduction

Carbon fiber reinforced plastics (CFRP) are composite materials characterized by their high strength, high stiffness, low thermal expansion, and lightweight properties [1, 2]. The

demand for CFRP has been recently increasing in various fields, such as aircraft, automotive, and space, driven by the need to improve fuel efficiency through weight reduction [3, 4]. Accordingly, the demand for precision machining of CFRP has also been rising.

However, CFRP is a challenging material to machine with high precision due to its substantial anisotropy in mechanical and thermal properties, depending on fiber direction. This anisotropy affects the shape and dimensional accuracy after machining. Therefore, traditional machining methods of CFRP, such as mechanical machining and cutting, often lead to a series of problems, including carbon fiber pull-out, delamination [5], excessive tool wear [6], abrasive penetration [7], and difficulties with abrasive slurry disposal [8,

✉ Jiwang Yan
yan@mech.keio.ac.jp

¹ School of Integrated Design Engineering, Graduate School of Science and Technology, Keio University, Yokohama 223-8522, Japan

² Department of Mechanical Engineering, Faculty of Science and Technology, Keio University, Yokohama 223-8522, Japan

9]. Aiming to address these problems, laser irradiation has been increasingly used for machining CFRP. Laser irradiation is a noncontact process, eliminating problems related to tool wear and surface tearing. In addition, laser irradiation enables the processing of complex shapes over large areas in a short time. The demand for fine drilling of CFRP has also increased in recent years, as laser drilling is crucial in various applications, such as noise reduction [10], the installation of fiber-optic sensors [11], and the joining of components [12].

However, reports revealed that when lasers with longer pulse durations, such as CW lasers or pulsed lasers with longer durations than nanoseconds, are used, the heat-affected zone (HAZ) in CFRP becomes larger, resulting in reduced processing accuracy compared to ultrashort pulsed lasers such as picosecond and femtosecond pulsed lasers [13, 14]. Therefore, laser ablation using ultrashort pulsed lasers is considered effective because it minimizes thermal effects. Salama et al. successfully drilled circular holes in CFRP using picosecond pulsed laser irradiation [15]. In recent years, many other researchers have also focused on picosecond pulsed laser irradiation for drilling and grooving applications [16, 17]. Femtosecond lasers, as ultrashort pulsed lasers with stronger peak power density and shorter pulse widths than picosecond lasers, have been shown to exhibit minimal heat dissipation and excellent controllability during their interactions with solid materials. This condition is due to the termination of the ablation process prior to thermal diffusion around the irradiated area. Notably, the time required for a material surface to reach high temperature and pressure, for heat conduction to spread to the periphery, and for thermal equilibrium to be reached is several tens of picoseconds [18]. The femtosecond scale is smaller than the aforementioned; thus, removing the material before heat conduction spreads to the periphery is possible. Therefore, femtosecond pulsed lasers are highly effective for processing a wide range of difficult-to-machine materials, including CFRP. However, most previous studies on laser processing of CFRP have focused on the fabrication of macroscale grooves and holes with feature sizes in the millimeter scale or larger. The micromachining behavior of submillimeter-sized features in CFRP has rarely been investigated. Such micro features are increasingly required in fields such as electronics and sensors. As the feature size decreases to the submillimeter range, the effects of CFRP anisotropy in thermal and mechanical properties, as well as the differences in laser machining mechanisms between carbon fibers and plastic, may become more pronounced. These factors can strongly influence the achievable form accuracy and surface quality. Therefore, a systematic and in-depth study on the mechanisms of femtosecond pulsed laser micromachining of CFRP submillimeter features is highly demanded in industry and academia.

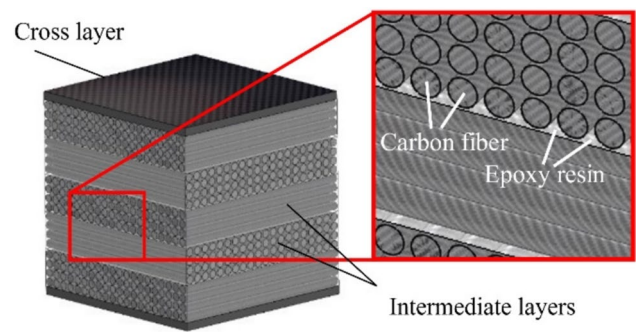


Fig. 1 Laminate structure of CFRP

Furthermore, most previous studies on the laser processing of CFRP have focused on circular drilling using a laser beam with a large spot diameter [9], while drilling rectangular holes with sharp corners in CFRP has not yet been realized. In particular, laser micromachining of submillimeter square holes remains unresolved. Such microscale rectangular holes hold considerable potential for the direct mounting and attachment of various micro sensors and IC chips onto CFRP substrates without using screws or glues. This study introduces a femtosecond pulsed laser micromachining of CFRP using a small-diameter laser beam to fabricate submillimeter-sized grooves and rectangular holes with sharp corners and investigate the fundamental processing characteristics. The success of this study will expand the possibility of fabricating three-dimensional microstructures and surface features on CFRP, which are increasingly required across various industries.

2 Experimental Procedures

The laser used in this study was a Yb: KGW laser PHAROS-08–600-PP, manufactured by Light Conversion, UAB, Lithuania. The laser operated at a wavelength of 1028 nm with a pulse width of 256 fs and a repetition frequency of 100 kHz. The laser spot had a circular diameter of 16 μm at the focal point, with a focal length of 70 mm. The laser beam displayed a Gaussian energy distribution and was linearly polarized. A galvanometer scanner system was used to control the X- and Y-axis scanning of the laser beam, with a laser motion program created using WinLase Professional software. The workpiece was placed on a Z-axis stage, and the laser beam was focused onto the workpiece surface using an f θ lens. The pulse interval and overlap were adjusted by varying the laser scanning speed, which ranged from 200 to 800 mm/s. The laser output was precisely controlled by the laser oscillator and the attenuator [19]. The CFRP used for the experiment was a 1.4 mm thick plate with an internal structure of six unidirectional CFRP layers,

as shown in Fig. 1. The CFRP has a stacked structure with intersecting layers stacked at 90° each. The type of carbon fiber was PAN-based, with a fiber diameter of approximately $6\ \mu\text{m}$, and the surface cross-layer comprised approximately 3000 carbon fibers per bundle. The surface cross layer is $140\text{--}250\ \mu\text{m}$ thick, and each intermediate layer is $90\text{--}450\ \mu\text{m}$ thick. The CFRP plates used are made of prepreg, an intermediate material where carbon fibers are impregnated with resin and then pressurized, heated, and vacuumed in an autoclave to form the plates. The experimental conditions are shown in Table 1, and the experimental equipment is presented in Fig. 2. The polarization direction of the laser beam is aligned with the x -axis, as depicted in Fig. 2. The

Table 1 Laser irradiation condition

Laser medium	Yb: KGW
Wavelength λ [nm]	1028
Spot diameter [μm]	16
Pulse width [fs]	256
Repetition frequency [kHz]	100
Fluence [J/cm^2]	1.0–8.5
Scanning speed [mm/s]	25–800
Number of irradiations	1–370

irradiation method for planar irradiation is shown in Fig. 3. Blind hole and through-hole drilling were attempted using circular irradiation with a radius of $0.5\ \text{mm}$, as well as square irradiation with side lengths of 0.5 or $1\ \text{mm}$. During through-hole drilling, the focus was adjusted by elevating the sample stage in the Z -direction to compensate for changes in the focal point relative to the material surface. The sample stage was manually raised by $100\ \mu\text{m}$ after every 10 cycles of laser irradiation.

After laser irradiation, the surface and hole walls of the samples were observed using a scanning electron microscope (SEM), Inspect F50, made by FEI Company, USA. The depth of the irradiated area, as well as the profile of the grooves and holes, were measured using a shape analysis laser microscope, VK-X1000, from Keyence Corporation, Japan. For quantitative analysis, the heat-affected zone (HAZ) was calculated through image analysis using image processing software [20]. SEM images were imported into the software to visually measure the areas where the resin surface was damaged, such as regions where carbon fibers were exposed, or cracks appeared in the resin.

Fig. 2 Experimental setup for laser irradiation

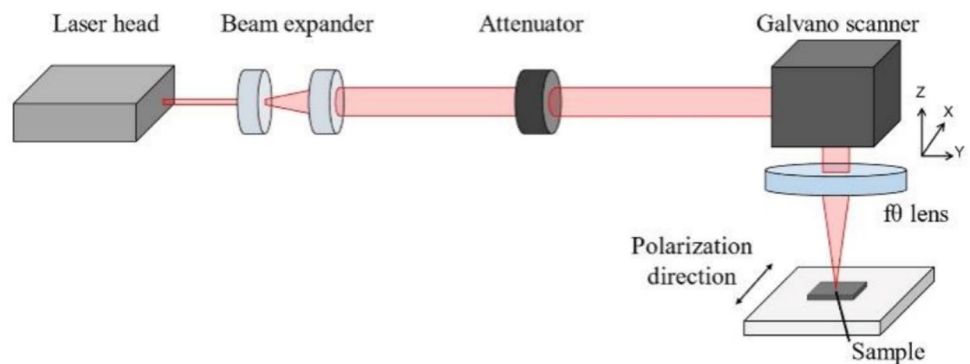


Fig. 3 Laser scanning method for drilling: **a** Circle; **b** Square

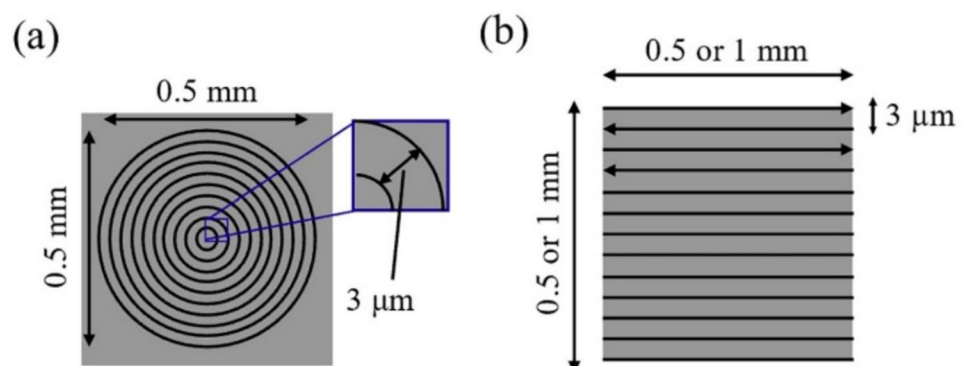
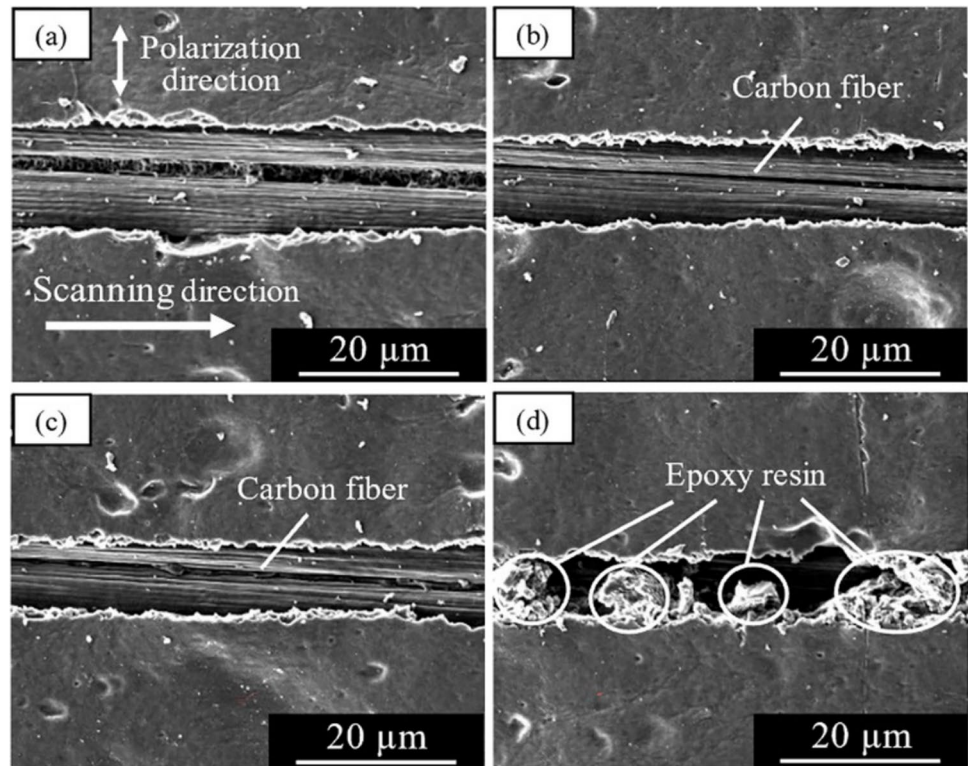


Fig. 4 SEM images of micro-grooves with different laser scanning speeds: **a** 200 mm/s, **b** 400 mm/s, **c** 600 mm/s, and **d** 800 mm/s



3 Results and Discussion

3.1 Effect of Laser Scanning Speed

Line irradiation was conducted by changing the scanning speed in increments of 200 mm/s, within the range of 200–800 mm/s. The number of irradiation was fixed at 1 time with a fluence of 1.8 J/cm². The surface of the material was observed using SEM. Figure 4 shows the SEM image of the surface after irradiation. The width of the grooves increased as the scanning speed decreased. This finding is possibly due to an increase in the overlap rate of the pulses and a corresponding increase in the amount of heat delivered to the material as the scanning speed decreased [21]. The overlap rate of the laser pulses η can be expressed as shown in Eq. (1):

$$\eta = \frac{2 \left[r^2 \cos^{-1} \left(\frac{l}{2r} \right) - \frac{l}{2} \sin \left\{ \cos^{-1} \left(\frac{l}{2r} \right) \right\} \right]}{\pi r^2} \quad (1)$$

where r is the laser spot radius, and l is the distance between the centers of laser pulses, which can be expressed as in Eq. (2):

$$l = \frac{v}{f} \quad (2)$$

where v is the scanning speed, and f is the repetition frequency. As shown in Eqs. (1) and (2), the scanning speed

is a crucial factor affecting the laser pulse overlap rate, which is strongly associated with thermal damage to the material [22]. Therefore, the increase in overlap due to the reduction in scanning speed resulted in an increase in groove width. Grooves with clear edges were obtained at scanning speeds of 400–600 mm/s. However, the edges of the work traces became unclear at scanning speeds of 200 and 800 mm/s, and more debris was observed at a scanning speed of 800 mm/s. The number of pulses at the irradiation spot increased with a reduction in scanning speed. Thus, the removal of debris was attributed to heat accumulation caused by overlapping laser pulses. The debris observed herein was considered to be epoxy resin, which had once vaporized and was re-solidified on the material surface via air cooling [23]. Therefore, a scanning speed of 400–600 mm/s is necessary to sufficiently remove debris and obtain a clear edge. Based on Eq. (1), the overlap rates between pulses are approximately 69% and 39% at scanning speeds of 400 and 800 mm/s, respectively. Therefore, at a scanning speed of 800 mm/s, where the overlap rate notably decreased, the heat required to completely remove the re-deposited debris is not achieved.

3.2 Effect of Laser Fluence

Line irradiation was performed at a scanning speed of 400 mm/s, with the number of irradiations set at 10, while changing laser fluences from 1.0 to 6.5 J/cm². The machined

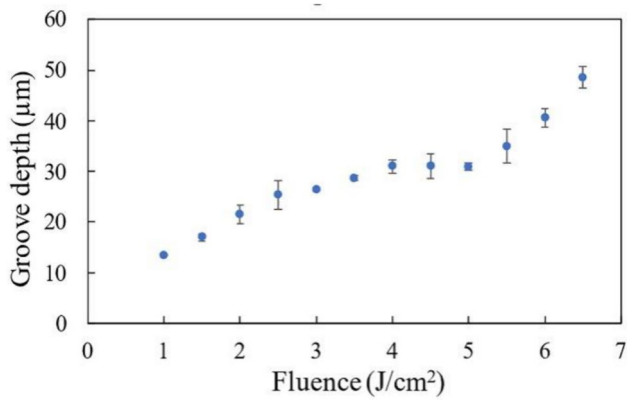


Fig. 5 Groove depth obtained at different laser fluences

surface and measurement of the groove depth were observed at different fluences. Figure 5 shows the groove depth at each fluence. The groove depth demonstrated an increasing tendency as the laser fluence increased. This increase is because the laser beam penetrates deeper into the material as the fluence increases, extending the range where ablation occurs and processing deeper grooves. Figure 6 shows the SEM images of grooves at laser fluences of 3.0–6.0 J/cm². At a fluence of 3.0 J/cm², carbon fibers in the same direction as the groove direction were observed on the bottom surface of the groove; at fluences of 4.0–5.0 J/cm², carbon

fibers in a direction perpendicular to the groove direction were observed. At a laser fluence of 6.0 J/cm², carbon fibers in the same direction as the groove direction were again observed on the bottom surface of the groove. These SEM images reveal the occurrence of this phenomenon during the transition of layers in CFRP with a laminated structure. The change in orientation of the carbon fibers during the layer transition and the change in direction of heat conduction may have temporarily reduced the amount of material removed in the depth direction via ablation.

3.3 Effect of the Angle Between Fiber Direction and Laser Scanning Direction

CFRP is an anisotropic material. Thus, the effect of the angle between the laser scanning direction and the carbon fiber direction on the processing characteristics was investigated. Using the irradiation method presented in Fig. 3 (a), the laser was irradiated in a circular pattern from the inside to the outside at a scanning speed of 400 mm/s and a fixed fluence of 5.0 J/cm² while adjusting the focus position every 10 irradiation cycles. A circular through-hole with a diameter of approximately 0.5 mm was drilled by performing 220 times of laser irradiation in total. Figure 7 shows SEM images of the wall of the circular through-hole. As the angle between the scanning and carbon fiber directions approached 90°, the wall surface

Fig. 6 SEM images of micro-grooves fabricated by laser irradiation at different fluences: **a** 3.0 J/cm², **b** 4.0 J/cm², **c** 5.0 J/cm², and **d** 6.0 J/cm²

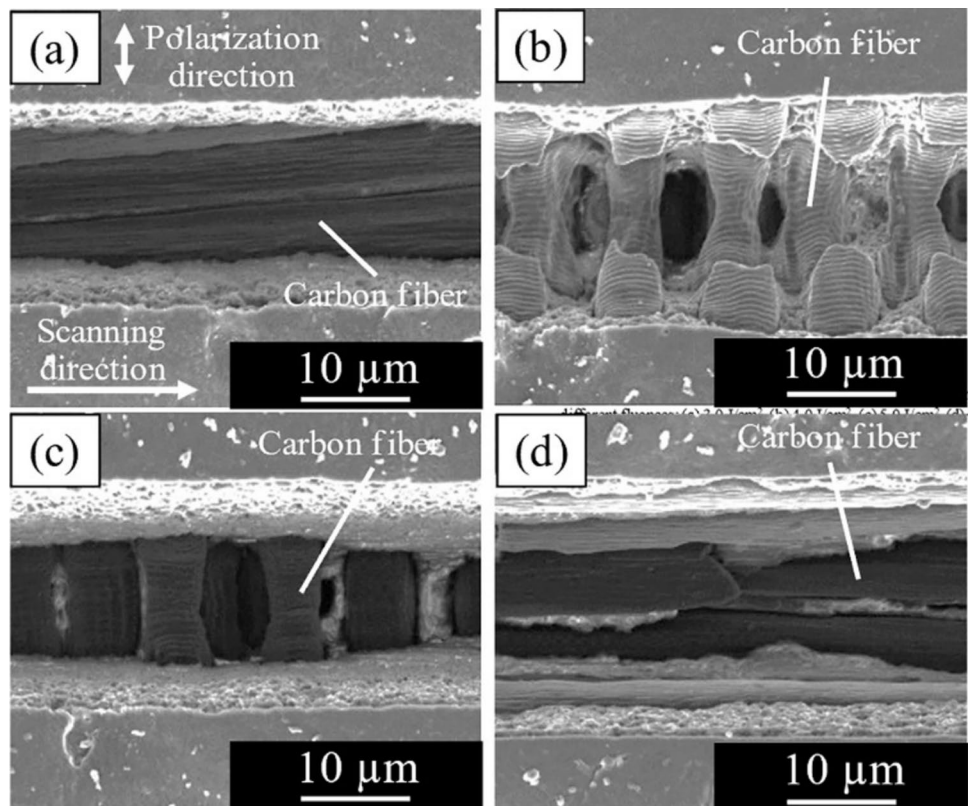
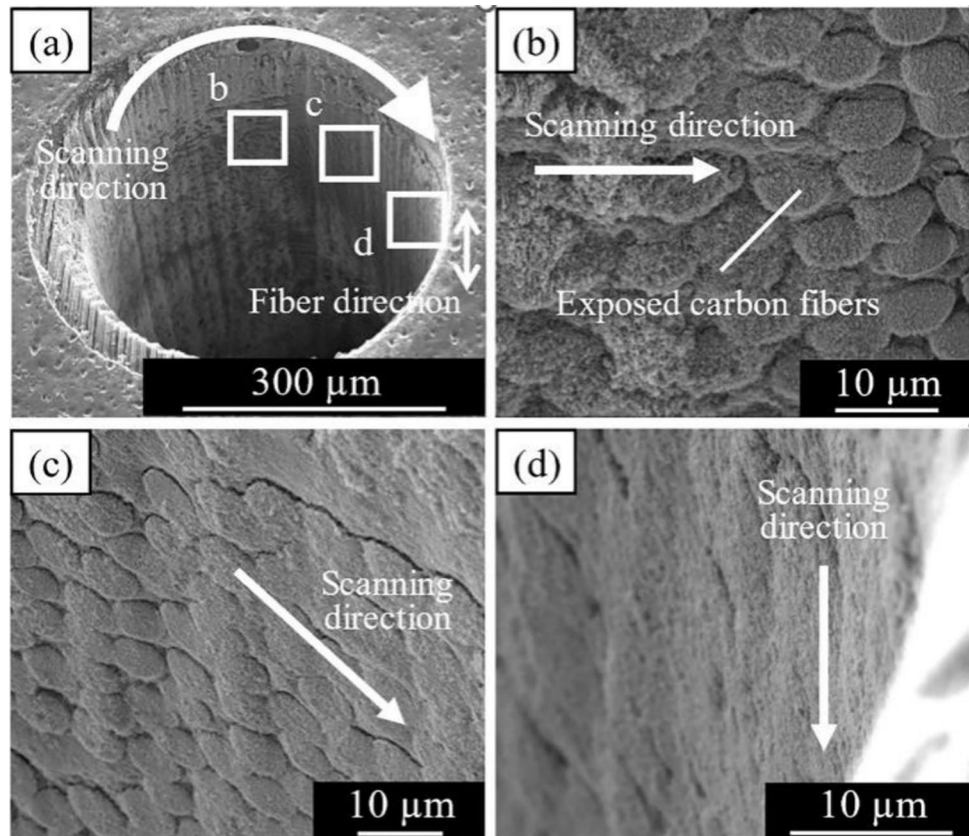


Fig. 7 SEM images of a circular through-hole: **a** Whole image; **b** 90° layer; **c** 45° layer; **d** 0° layer



became highly uneven, and an increase in exposed carbon fibers was observed on the wall surface. This finding is believed to be attributed to the relationship between the carbon fiber direction and thermal conductivity of CFRP. Carbon fiber exhibits high thermal conductivity in the carbon fiber direction, which is substantially higher than that of resin [24]. The difference in the ablation threshold between epoxy resin and carbon fiber facilitates the easier ablation of epoxy resin compared to carbon fiber. As shown in Fig. 8, epoxy resin is removed first, followed by carbon fiber. During this process, resin evaporation around the carbon fiber occurs due to thermal conduction in the

carbon fiber direction, and even the resin around the fiber other than the laser-irradiated area is also removed [25, 26].

3.4 Rectangular Blind Hole Drilling

Rectangular blind-hole drilling experiments were conducted to investigate the effect of heat conduction in the carbon fiber direction on the edges of the machining trace after drilling a deep hole by laser irradiation. The scanning speed was varied between 25 and 500 mm/s, and the laser was irradiated 5–10 times with a fluence ranging from 1.0 to 5.0 J/cm²

Fig. 8 Schematic of material removal via heat conduction in the direction of carbon fibers

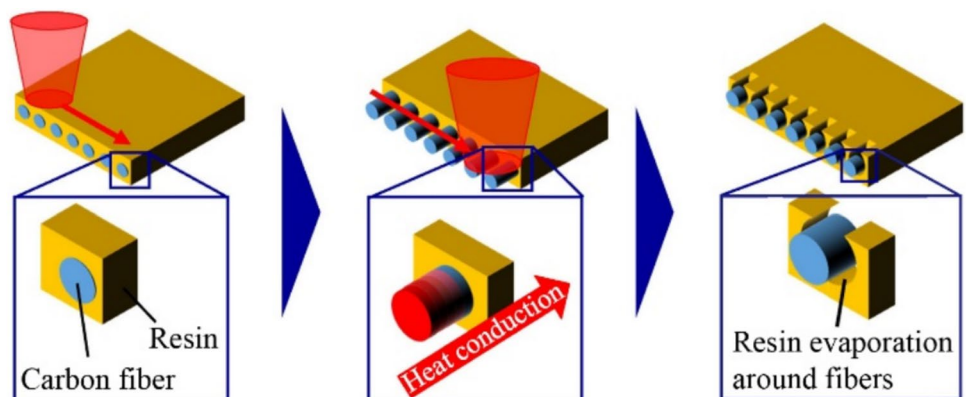
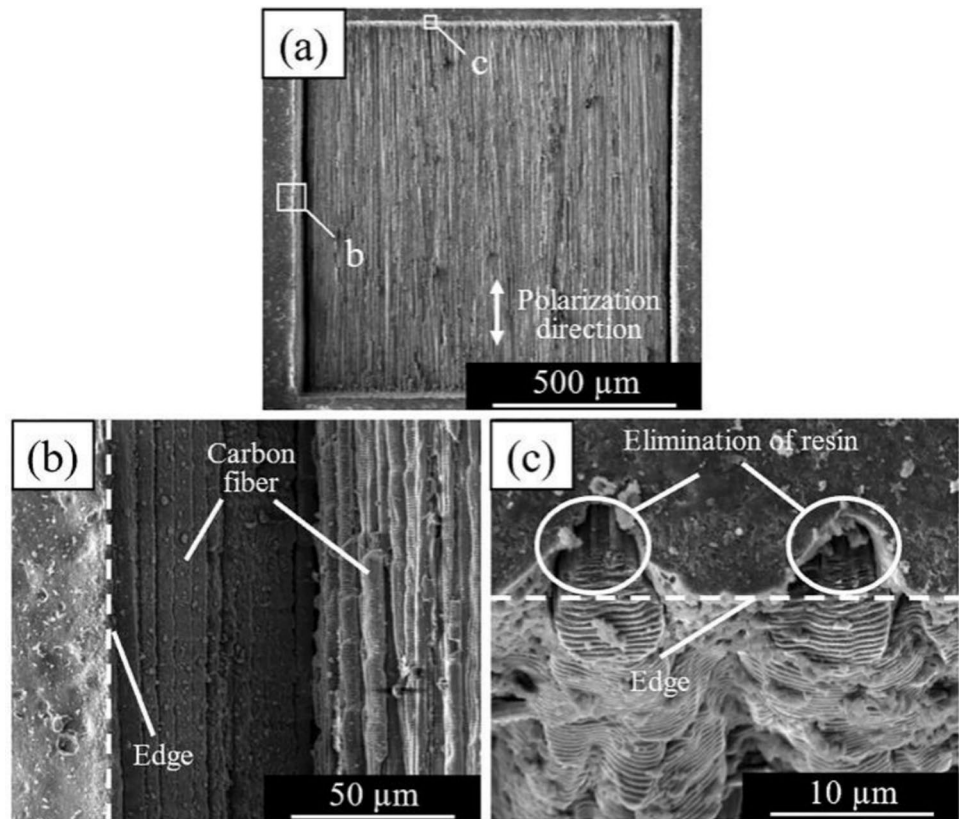


Fig. 9 SEM images of a rectangular blind hole (Scanning speed: 400 mm/s, fluence: 3.0 J/cm², number of irradiations: 10 times): **a** Whole image; **b** Edge parallel to the scanning direction; **c** Hole edge perpendicular to the scanning direction



and a hatch width of 3 μm. Figure 9 shows SEM images of the edges of the rectangular blind hole. Resin evaporation was observed along the carbon fibers at the edge of the trace. The edges parallel to the carbon fiber direction formed sharp edges, while the edges perpendicular to the carbon fibers showed resin evaporation removal from the surface of the material along the carbon fiber orientation.

A HAZ was defined to quantitatively evaluate the thermal damage to the edge of the machining trace. As shown in Fig. 10, in this study, the HAZ was defined as the area where processing actually occurred minus the ideal processing area through which the laser spot passed. Since the laser spot was programmed to trace a square of 500 × 500 square micrometers at its center, the ideal machined area in this experiment is 516 × 516 square micrometers, as shown in Fig. 10 (a). The area where processing actually occurred refers to the region where the surface resin was damaged, as shown in Fig. 10 (b). Thermal damage increases as the angle between the fiber and scanning directions approaches 90°, as discussed in Sect. 3.3. Figure 11 shows the HAZ for the rectangular blind hole, with edges parallel and perpendicular to the carbon fiber. The HAZ was larger when the edge was perpendicular to the fiber direction compared to when the edge was parallel to the fiber direction. As presented in the previous section, CFRP has a high thermal conductivity in the carbon fiber direction, which is believed to be attributed

to resin evaporation around the carbon fiber due to thermal conduction in the carbon fiber direction.

3.5 Rectangular Through-Hole Drilling

Rectangular through-hole drilling experiments were conducted with the scanning speed set to 400 mm/s. The fluence was 5.0 J/cm² for 1–50 irradiations and 8.5 J/cm² for 51–370 irradiations, totaling 370 irradiations with focus position adjustments. Therefore, a rectangular through-hole was successfully drilled.

The whole SEM image of the rectangular through-hole is shown in Fig. 12 (a), and an enlarged SEM image of the corner of the hole is shown in Fig. 12 (b). The 3D images and cross-sectional profiles of the hole sidewalls, measured at points c, d, e, and f, are shown in Fig. 12 (c), (d), (e), and (f), respectively. All the cross-sectional profiles reveal similar curves with a gradually increasing taper angle.

In this study, the taper angle refers to the angle between the horizontal line and the slope line that connects the hole edge at the top surface to the hole edge at the bottom surface in the hole cross-section. The taper angles on both side walls were approximately 100°. The gradual increase in taper angle with hole depth is due to the reduction in laser fluence in the deeper part of the hole. The incident laser beam, shielded by the upper slope surface, leads to the expansion

Fig. 10 Definition of HAZ: **a** Definition of ideal processed area; **b** Definition of actual processed area (The area enclosed by yellow dotted line indicates actual processed area, while the area enclosed by blue dotted line indicates ideal processed area)

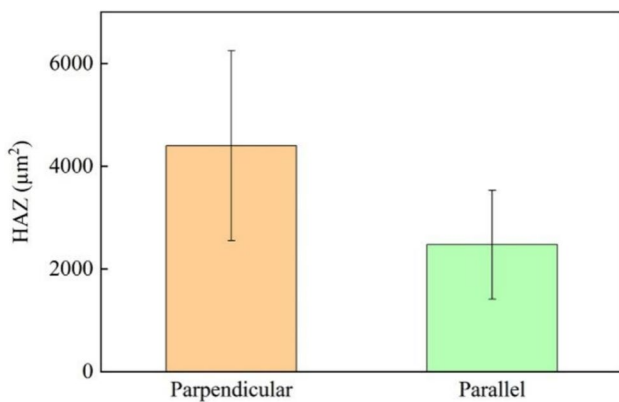
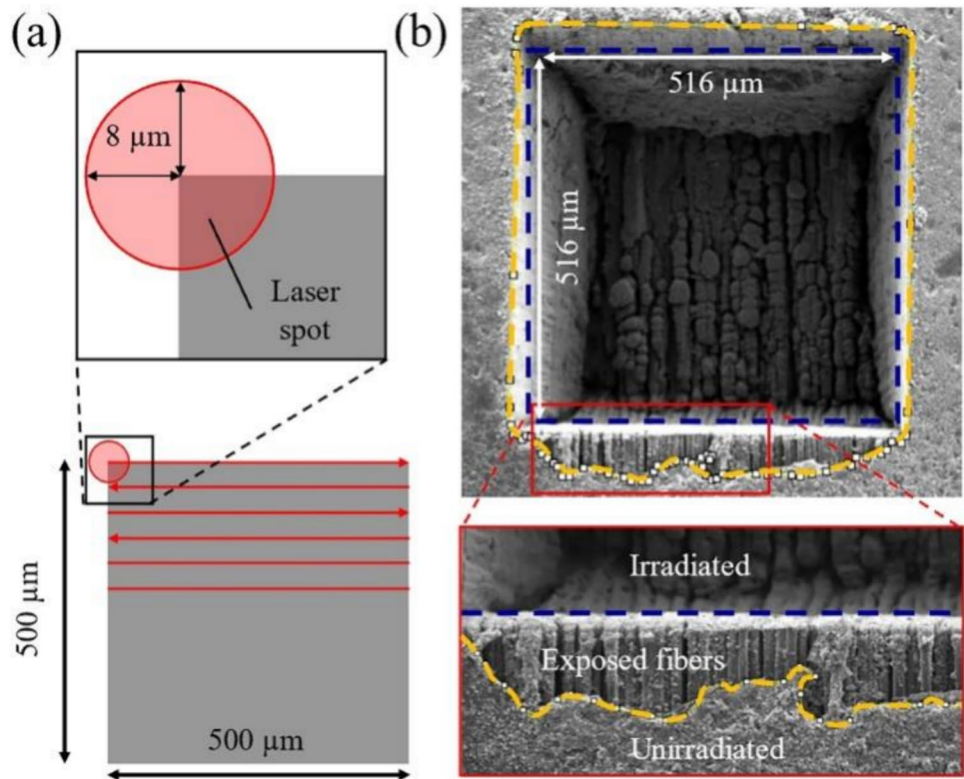


Fig. 11 HAZ for the rectangular blind hole with the edge parallel and perpendicular to the carbon fibers

of the focused spot area along the sidewall in the deeper area of the hole. This phenomenon results in a reduction in laser fluence in deeper areas and an increase in taper angles [27]. Furthermore, considering the Gaussian intensity distribution, the laser intensity near the center of the laser spot is stronger than at locations away from the center, and additional materials were removed near the center of the laser spot, leading to an increase in taper angle [28]. As shown in Fig. 12 (b), grooves were also observed at the hole corners where the sidewalls intersected each other. This finding is

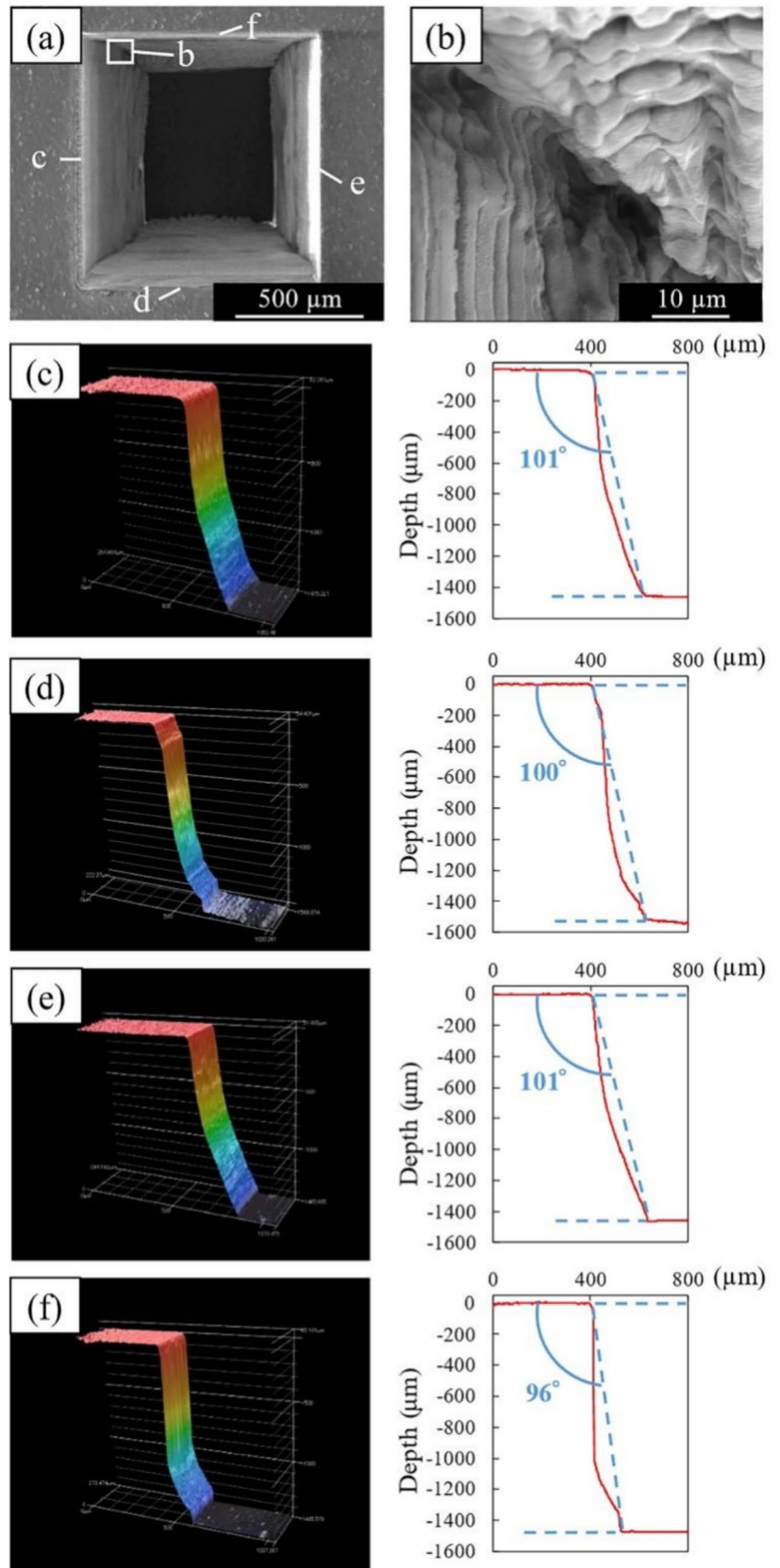
believed to be due to the decrease in the laser scanning speed near the start and end points of the laser scanning, which increases the overlap rate between the laser pulses. Notably, the spot diameter of the laser beam used in this experiment (16 μm) was the smallest spot diameter at the focal point. Achieving a smaller spot diameter using the present experimental setup is challenging. However, using an objective lens with a smaller focal length could allow for a smaller spot diameter, enabling the drilling of rectangular holes with substantially sharper corners.

4 Conclusions

Femtosecond pulsed laser irradiation was performed on CFRP to investigate the fundamental micro-grooving and drilling characteristics. The following conclusions were obtained:

- Line irradiation formed microscale grooves, and clear-edged grooves were obtained at scanning speeds ranging from 400 to 600 mm/s.
- The groove depth increased with laser fluence. The increase in groove depth is considered to have decreased at the transition between CFRP layers.
- A microscale circular through-hole was fabricated through circular surface irradiation. As the angle between

Fig. 12 Laser-drilled rectangular through hole: **a** Whole SEM image; **b** Enlarged SEM image of the corner of the hole; **c** 3D image and cross-sectional profile of the left sidewall; **d** 3D image and cross-sectional profile of the lower sidewall; **e** 3D image and cross-sectional profile of the right sidewall; **f** 3D image and cross-sectional profile of the upper sidewall



the carbon fiber direction and the laser scanning direction approached 90°, the hole wall surface became increasingly uneven.

- Microscale rectangular blind holes and a through-hole were fabricated through rectangular surface irradiation. In areas where the fiber direction was perpendicular to the hole edge, results revealed that even the resin on the surface of the material, away from the irradiated area, was removed due to thermal conduction along the fiber direction.

These findings contribute to an improved understanding of the ultrashort pulsed laser processing characteristics and mechanisms in CFRP. They also demonstrate the potential for drilling high-precision holes and creating other three-dimensional microstructures, which are useful in direct bonding and fixing of sensors/IC chips to CFRP substrates.

Author contributions Both authors read and approved the final manuscript.

Data Availability Statement There is no data associated with the manuscript.

Declarations

Competing interest Jiwang Yan is an editorial board member for "Nanomanufacturing and Metrology" and was not involved in the editorial review, or the decision to publish this article. The authors declare that they have no known competing financial interests or personal relationships that could have appeared to influence the work reported in this paper.

Open Access This article is licensed under a Creative Commons Attribution 4.0 International License, which permits use, sharing, adaptation, distribution and reproduction in any medium or format, as long as you give appropriate credit to the original author(s) and the source, provide a link to the Creative Commons licence, and indicate if changes were made. The images or other third party material in this article are included in the article's Creative Commons licence, unless indicated otherwise in a credit line to the material. If material is not included in the article's Creative Commons licence and your intended use is not permitted by statutory regulation or exceeds the permitted use, you will need to obtain permission directly from the copyright holder. To view a copy of this licence, visit <http://creativecommons.org/licenses/by/4.0/>.

References

- Li WY, Zhang GJ, Huang Y, Rong YM (2021) Drilling of CFRP plates with adjustable pulse duration fiber laser. *Mater Manuf Process* 36(11):1256–1263. <https://doi.org/10.1080/10426914.2021.1905838>
- Chen ML, Guo BS, Jiang L, Liu ZP, Qian Q (2023) Analysis and optimization of the heat affected zone of CFRP by femtosecond laser processing. *Optics Laser Technol* 167:109756. <https://doi.org/10.1016/j.optlastec.2023.109756>
- Li WY, Huang Y, Chen XH, Zhang GJ, Rong YM, Lu Y (2021) Study on laser drilling induced defects of CFRP plates with different scanning modes based on multi-pass strategy. *Optics Laser Technol* 144:107400. <https://doi.org/10.1016/j.optlastec.2021.107400>
- Li WY, Zhang GJ, Huang Y, Rong YM (2021) UV laser high-quality drilling of CFRP plate with a new interlaced scanning mode. *Compos Struct* 273:114258. <https://doi.org/10.1016/j.compstruct.2021.114258>
- Kim JD, Lee ES (1996) A study of ultrasonic vibration cutting of carbon fibre reinforced plastics. *Int J Adv Manuf Technol* 12(2):78–86. <https://doi.org/10.1007/BF01178947>
- Herzog D, Jaeschke P, Meier O, Haferkamp H (2008) Investigations on the thermal effect caused by laser cutting with respect to static strength of CFRP. *Int J Mach Tools Manuf* 48(12–13):1464–1473. <https://doi.org/10.1016/j.ijmactools.2008.04.007>
- König W, Wulf Ch, Graß P, Willerscheid H (1985) Machining of fibre reinforced plastics. *CIRP Ann* 34(2):537–548. [https://doi.org/10.1016/S0007-8506\(07\)60186-3](https://doi.org/10.1016/S0007-8506(07)60186-3)
- Jiang H, Ma CW, Li M, Cao ZL (2021) Femtosecond laser drilling of cylindrical holes for carbon fiber-reinforced polymer (CFRP) composites. *Molecules* 26(10):2953. <https://doi.org/10.3390/molecules26102953>
- Salama A, Yan YZ, Li L, Mativenga P, Whitehead D, Sabli A (2016) Understanding the self-limiting effect in picosecond laser single and multiple parallel pass drilling/machining of CFRP composite and mild steel. *Mater Design* 107:461–469. <https://doi.org/10.1016/j.matdes.2016.06.048>
- Staehr R, Henzler M, Wippo V, Jaeschke P, Kaierle S, Overmeyer L (2022) Thermal process control for laser micro-drilling of thin CFRP-laminates. *High-power Laser Mater Process: Appl, Diagn Syst XI*. <https://doi.org/10.1117/12.2607494>
- Mishra YK, Mishra S, Jayswal SC (2021) Parametric analysis and optimization of inclined laser percussion drilling of carbon fiber reinforced plastic using solid-state Nd: YAG laser. *Lasers Manuf Mater Process* 8:325–354. <https://doi.org/10.1007/s40516-021-00151-5>
- Ramanujam N, Dhanabalan S, Kumar DR, Jeyaprakash N (2021) Investigation of micro-hole quality in drilled CFRP laminates through CO2 laser. *Arab J Sci Eng* 46(8):7557–7575. <https://doi.org/10.1007/s13369-021-05505-x>
- Jaeschke P, Stolberg K, Bastick S, Ziolkowski E, Roehner M, Suttman O, Overmeyer L (2014) Cutting and drilling of carbon fiber reinforced plastics (CFRP) by 70W short pulse nanosecond laser. *High-Power Laser Mater Process: Lasers, Beam Deliv, Diagn Appl III*. <https://doi.org/10.1117/12.2036086>
- Sato Y, Tsukamoto M, Matsuoka F, Yamashita K, Takahashi K, Masuno S (2015) Experimental investigation of CFRP cutting with nanosecond laser under air and Ar gas ambience. *Laser Appl Microelectron Optoelectron Manuf (LAMOM) XX*. <https://doi.org/10.1117/12.2078645>
- Salama A, Li L, Mativenga P, Sabli A (2016) High-power picosecond laser drilling/machining of carbon fibre-reinforced polymer (CFRP) composites. *Appl Phys A*. <https://doi.org/10.1007/s00339-016-9607-8>
- Herrmann T, Stolze M, L'huillier J, (2014) Laser drilling of carbon fiber reinforced plastics (CFRP) by picosecond laser pulses: Comparative study of different drilling tools. *Front Ultrafast Optics: Biomed, Sci Indus Appl XIV*. <https://doi.org/10.1117/12.2039077>
- Li JY, Ding Y, Ge CC, Sun XY, Yang LJ, Wang Y, Zhang W, Lu YQ (2023) Investigations on 355 nm picosecond laser machining of carbon fiber reinforced polymer composites. *J Manuf Process* 101:854–866. <https://doi.org/10.1016/j.jmapro.2023.06.036>
- Luk'yanchuk B, Bituryn N, Malyshev A, Anisimov S, Arnold N, Bauerle D (1998) Photophysical ablation. *High-Power Laser Ablat* 3343:58–68. <https://doi.org/10.1117/12.321601>
- Yamamuro Y, Shimoyama T, Yan J (2023) Generation of nanopore structures in yttria-stabilized zirconia by femtosecond pulsed laser

- irradiation. *J Mater Res and Technol* 23:1155–1176. <https://doi.org/10.1016/j.jmrt.2023.01.079>
20. Rasband W S, ImageJ, U. S. National Institutes of Health, Bethesda, Maryland, USA, <http://rsb.info.nih.gov/ij/>, 1997–2012.
 21. Chaja M, Kramer T, Neuenschwander B (2018) Influence of laser spot size and shape on ablation efficiency using ultrashort pulse laser system. *10th CIRP Conf Photon Technol* 74:300–304. <https://doi.org/10.1016/j.procir.2018.08.119>
 22. Wang P, Zhang Z, Hao B, Wei SC, Qiu WZ, Huang Y, Zhang GJ (2023) Study on anisotropic heat transfer and thermal damage in nanosecond pulsed laser processing of CFRP. *Polym Compos* 44(9):5964–5983. <https://doi.org/10.1002/pc.27540>
 23. Nakajima A, Yan JW (2022) Response of resin coating films containing fine metal particles to ultrashort laser pulses. *Int J Precision Eng Manuf* 23(4):385–393. <https://doi.org/10.1007/s12541-022-00629-y>
 24. Tao NR, Chen GY, Fan LC, Wang BA, Li MQ, Fang WJ (2021) Temperature-dependent material removal during pulsed laser processing of CFRP composites. *Opt Laser Technol* 144:107445. <https://doi.org/10.1016/j.optlastec.2021.107445>
 25. Oliveira V, Sharma SP, de Moura MFSF, Moreira RDF, Vilar R (2017) Surface treatment of CFRP composites using femtosecond laser radiation. *Optic Lasers Eng* 94:37–43. <https://doi.org/10.1016/j.optlaseng.2017.02.011>
 26. Weber R, Hafner M, Michalowski A, Graf T (2011) Minimum damage in CFRP laser processing. *Phys Procedia* 12(part B) 12:302–307. <https://doi.org/10.1016/j.phpro.2011.03.137>
 27. Tao NR, Chen GY, Fang WJ, Li MQ (2023) Understanding the bowl-bottom effect in ultra-short pulsed laser drilling of CFRP laminate. *Compos Struct* 305:116498. <https://doi.org/10.1016/j.compstruct.2022.116498>
 28. Zhang YM, Shen ZH, Ni XW (2014) Modeling and simulation on long pulse laser drilling processing. *Int J Heat Mass Trans* 73:429–437. <https://doi.org/10.1016/j.ijheatmasstransfer.2014.02.037>



Yuhei Konishi received his bachelor's degree in mechanical engineering from Keio University in 2023. He is currently a master's degree graduate student in integrated design engineering at Keio University under supervision of Prof. Jiwang Yan. His research interests are laser processing and precision machining.



Jiwang Yan received his Ph.D. from Tohoku University, Japan in 2000 and is currently a professor of Mechanical Engineering at Keio University (2012–now), leading the Laboratory for Precision Machining and Nano Processing. His research areas include ultraprecision machining, micro/nano manufacturing, laser processing, nanomaterials, and nanomechanics.